Journal of Instrumentation

PAPER

Computational approaches to Coherent Synchrotron Radiation in two and three dimensions

J inst

Published by IOP Publishing for Sissa Medialab

Received: *August 10, 2021*
Accepted: *September 11, 2021*
Published: *October 11, 2021*

ICFA Beam Dynamics Newsletter#82 — Advanced Accelerator Modelling

Computational approaches to Coherent Synchrotron Radiation in two and three dimensions

C.E. Mayes

SLAC National Accelerator Laboratory,
Menlo Park, CA, 94025, U.S.A.

E-mail: cmayes@stanford.edu

Abstract: Coherent Synchrotron Radiation (CSR) is an important and often detrimental effect in particle accelerators. While one-dimensional models have been successfully used to design and explain the behavior of modern machines, questions remain about their domain of validity. In recent years, two- and three-dimensional models have been developed that are amenable to efficient numerical computation. This article gives an overview of CSR computation from its discovery through the present state of the art.

Keywords: Accelerator modelling and simulations (multi-particle dynamics, single-particle dynamics); Beam dynamics; Coherent instabilities; Simulation methods and programs

https://doi.org/10.1088/1748-0221/16/10/P10010

Contents

1 **Introduction** 1

2 **Early history** 2

3 **CSR Wakefield** 4
- 3.1 Basic approaches 4
- 3.2 One-dimensional analytic models 5
- 3.3 Two- and three-dimensional analytic models 7

4 **Numerical computation** 10
- 4.1 One-dimensional numerical approaches 10
- 4.2 Field-based numerical approaches 10
- 4.3 Two-dimensional particle-based numerical approaches 11
- 4.4 Three-dimensional particle-based numerical approaches 12

5 **Outlook** 15

1 Introduction

The theory of charged particles moving on a circle was first studied in the early 1900s as an attempt to explain atomic spectral lines. In the 1940s physicists worried that overall energy loss due to coherent effects would limit the operation of future particle accelerators, which led to great development in theory and the experimental discovery of synchrotron radiation (SR). The subject eventually gave birth to an entirely new field of photon science. A good summary of these developments and many references can be found in an earlier Newsletter [1].

In the 1990s plans for strong longitudinal bunch compression in free electron lasers (FELs) and linear colliders motivated the development of one-dimensional models for the self-effect of coherent synchrotron radiation (CSR). While these models have served the community well and agree with important measurements [2], questions remain about their domain of validity. The transverse force first introduced by Talman [3], for example, is still debated among experts. Today ideas for even stronger compression (for example, to probe non-perturbative quantum electrodynamics [4]), and the opportunities to measure their effects [5] have motivated new work in developing models for CSR in two- and three-dimensions [6–11].

This article focuses on the computational aspects of the self-effect of the CSR on the source particles. In the early days physicists relied on their knowledge of special functions, numerical approximations, and symbolic manipulations to derive useful analytic expressions. Today we also rely on high-performance computing and efficient numerical techniques to go beyond what can be written in closed form.

2021 JINST 16 P10010

2 Early history

The electromagnetic field produced by an accelerated charged particle has been of fundamental importance to physics for well over a century now. The power radiated by such a particle was first calculated by Larmor in 1897 [12], with Liénard deriving the first relativistically correct version in 1898 [13]. In non-covariant form, this power is

$$P = \frac{2}{3}\frac{r_c\, m}{c}\gamma^4 \left(\dot{\boldsymbol{\beta}}^2 + \gamma^2 \boldsymbol{\beta}\cdot\dot{\boldsymbol{\beta}}\right), \tag{2.1}$$

in which $\boldsymbol{\beta}$ and $\dot{\boldsymbol{\beta}}$ are the velocity and acceleration vectors relative to the speed of light c, respectively, m is the mass, r_c is the classical electromagnetic radius, $\gamma = (1-\beta^2)^{-1/2}$ is the Lorentz factor of the particle, and $\beta = |\boldsymbol{\beta}|$. For purely transverse acceleration this reduces to

$$P^{(1)} = \frac{2}{3}\frac{r_c\, m\, c^3\, \beta^4\, \gamma^4}{\rho^2}, \tag{2.2}$$

where ρ is the instantaneous radius of curvature.

The scaling with energy $\mathcal{E} = \gamma m c^2$ prompted Iwanenko & Pomeranchuk to note that this would ultimately limit the maximum energy attainable in a betatron accelerator [14]. However, it was known at the time that continuous currents do not radiate, and conversely that N closely spaced charged particles would radiate power coherently proportional to N^2. This dichotomy prompted Blewett in 1945 to search for energy losses experimentally in a 100 MeV betatron, who found that indeed the particles lose energy, but incoherently. At first he expected that the power would be within the first thousand harmonics, but looking at the microwave part of the spectrum he was unable to observe any radiation [15].

Perhaps forgotten at the time, the power spectrum of a particle moving on a circle had already been derived by Schott in his Adams Prize essay of 1909 [16]. Written in a time before the establishment of relativity and quantum mechanics, this work contains interesting discussions regarding various extended models of the electron, superluminal particle motion, and the influence of the æther. However, like Larmor and Liénard, he generally relies on the assumption that Maxwell's equations are correct. In examining the motion of a single particle moving in a circle of radius ρ he finds the spatial distribution of the radiated fields and, in particular, he finds that the electromagnetic power radiated in the n^{th} harmonic of the revolution frequency is

$$P_n^{(1)} = n\frac{2\,\beta\, c\, r_c\, m\, c^2}{\rho^2}\left[\beta^2 J'_{2n}(2n\,\beta) - n\left(1-\beta^2\right)\int_0^{\beta} J_{2n}(2n\,x)\,\mathrm{d}x\right], \tag{2.3}$$

in which J_n is the n^{th} Bessel function of the first kind. It was hoped that the origin of atomic spectral lines would be explained by such radiation, but this approach ultimately failed.

Meanwhile in late 1944 the problem had been introduced to Schwinger, who in 1945 performed detailed calculations of the spectrum. In a then-unpublished manuscript [17], he independently derives eq. (2.3) and, because it does not explicitly contain the dependence on γ that eq. (2.2) implies, he concludes that a great many harmonics must contribute to the total power. Using approximations for Bessel functions, he finds that

$$P_n^{(1)} \approx \frac{\sqrt{3}}{2\pi}\frac{\beta\, r_c\, m\, c^2}{\rho^2}\left(\frac{2n}{3}\right)^{1/3} \xi^{2/3}\int_{\xi}^{\infty} K_{5/3}(x)\,\mathrm{d}x \tag{2.4}$$

2021 JINST 16 P10010

with $\xi \equiv \frac{2n}{3\gamma^3}$, and K_n is a modified Bessel function of the second kind. The power is peaked around the critical harmonic $n_c \equiv \frac{3}{2}\gamma^3$.This can also be written as a power spectrum

$$\frac{dP^{(1)}}{d\omega}(\omega) = \frac{P^{(1)}}{\omega_c} S\left(\frac{\omega}{\omega_c}\right), \tag{2.5}$$

where ω is the angular frequency of the radiation, and $\omega_c \equiv \frac{3}{2}\gamma^3 c/\rho$ is the critical frequency [18]. The function S is defined as

$$S(\xi) \equiv \frac{9\sqrt{3}}{8\pi}\xi \int_\xi^\infty K_{5/3}(x)\,\mathrm{d}x, \tag{2.6}$$

where the integral $\int_0^\infty S(x)\,\mathrm{d}x = 1$, and therefore integrating over all frequencies recovers eq. (2.2).

Equation 2.5 is the form perhaps best known by modern physicists (see for example ref. [18]) as "synchrotron radiation" (SR), after its observation in 1947 in the General Electric 70 MeV synchrotron in Schenectady, New York. An account of the discovery, detailed by Pollock, notes that SR was originally referred to as "Schwinger radiation" based on their knowledge of his work [19]. While SR was readily used as an accelerator diagnostic, there was some question as to whether the classical calculations were valid [20]. Experiments using the 300 MeV synchrotron at Cornell University confirmed that they were, with the first accurate measurements of the energy loss in 1953 performed by Corson [21], and the first accurate measurements of the radiation spectrum in 1956 performed by Tomboullion & Hartman [22].

Schwinger went on to publish some of these results in 1949 [23], but the 1945 manuscript is pedagogically superior and continues with discussions of coherent effects with N particles moving on a circle. Following his arguments, it is straightforward to derive that a 'bunch' of N particles with a 1D distribution $\lambda(s)$ along path length s exhibits a power spectrum

$$\frac{dP^{(N)}}{d\omega}(\omega) \simeq \underbrace{N\frac{dP^{(1)}}{d\omega}}_{\text{incoherent}} + \underbrace{N(N-1)\left|\int \lambda(s)\exp\left(i\frac{\omega s}{\beta c}\right)\,\mathrm{d}s\right|^2 \frac{dP^{(1)}}{d\omega}}_{\text{coherent}}, \tag{2.7}$$

where $dP^{(1)}/d\omega$ is the single-particle power spectrum. The first term is the incoherent synchrotron radiation (ISR) and is independent of the bunch distribution, while the second term is CSR. The squared integral is called the form-factor and is responsible for greatly enhancing parts of the SR spectrum, depending on the bunch distribution.

For a Gaussian bunch distribution with standard deviation (bunch length) σ_z, the total power can be given in a closed form expression [24]. For short bunches at high energy, the average power lost per particle per unit distance is asymptotically

$$\left\langle \frac{P^{(N)}}{N\beta c} \right\rangle_{\text{coh.}} \sim \frac{\Gamma\left(\frac{5}{6}\right)}{6^{1/3}\sqrt{\pi}} \frac{N r_c m c^2}{\rho^{2/3}\sigma_z^{4/3}}, \tag{2.8}$$

where the numerical coefficient[1] $\Gamma(5/6)\,6^{-1/3}\,\pi^{-1/2} \simeq 0.350$. Schwinger originally derived a similar expression for a uniform bunch, which for the equivalent standard deviation has numerical

[1]Note that $\Gamma(5/6)\,6^{-1/3}\,\pi^{-1/2} = 3^{1/6}\Gamma(2/3)^2/(2\pi)$ which is sometimes reported in the literature.

coefficient $2^{-4/3} \simeq 0.397$. Note that while the power lost in eq. (2.8) increases with shorter bunches, it is independent of energy, unlike eq. (2.2). For this reason, CSR is not generally a limitation for reaching high energies in a particle accelerator.

Most particle accelerators have conducting beam chambers that naturally suppress the propagation of long wavelengths. If h is the characteristic size of this chamber, then roughly speaking wave numbers $k = \omega/c \lesssim 1/h$ should be strongly suppressed. This is called the "shielding" effect. The final section of ref. [17] shows that, at high energy, the average power lost per particle per unit distance for a uniform distribution[2] between two perfectly conducting parallel plates is

$$\left\langle \frac{P^{(N)}}{N\beta c} \right\rangle_{\text{coh.p.p.}} \sim \frac{\sqrt{3}}{24} \frac{N r_c m c^2 h}{\rho^2 \sigma_z^2}, \tag{2.9}$$

where h is the separation of the plates. This is of the same form as eq. (2.8) but with an additional shielding factor

$$b \equiv \frac{h}{\rho^{1/3} \sigma_z^{2/3}}. \tag{2.10}$$

The effect of shielding is important when $b \lesssim 3$ [25]. This work was continued in 1954 by Nodvick & Saxon [26].

3 CSR Wakefield

From energy conservation, the energy that goes into CSR must be the same as that lost by the particles producing it. Geometrically as the bunch moves on an arc, photons emitted by particles in the back of the bunch are able to interact with particles in the front of the bunch. For relativistic bunches in free space, the primary effect is that the center and back of the bunch lose energy, while the head of the bunch actually gains some energy. The functional form of the total force on a particle due to the bunch as a whole is called the CSR wakefield.

3.1 Basic approaches

One approach to derive the CSR wakefield is to start with the Liénard-Wiechert potentials for a point particle with charge q, which imply that the electric field at any position $\mathbf{x}$ and time t can given in terms of the particle's position $\mathbf{r}(\tau)$, velocity $\boldsymbol{\beta}(\tau)c$, and acceleration $\dot{\boldsymbol{\beta}}(\tau)c$ as

$$\mathbf{E}(\mathbf{x}, t) = \frac{q}{4\pi\epsilon_0} \left[\underbrace{\frac{\mathbf{n} - \boldsymbol{\beta}}{\gamma^2 (1 - \boldsymbol{\beta}\cdot\mathbf{n})^3 R^2}}_{\text{velocity}} + \underbrace{\frac{\mathbf{n} \times \{(\mathbf{n} - \boldsymbol{\beta}) \times \dot{\boldsymbol{\beta}}\}}{c (1 - \boldsymbol{\beta}\cdot\mathbf{n})^3 R}}_{\text{acceleration}} \right]_{\tau = t - R/c}, \tag{3.1}$$

where $R = |\mathbf{R}|$, $\mathbf{R} = \mathbf{x} - \mathbf{r}(\tau)$, $\mathbf{n} = \mathbf{R}/R$, ϵ_0 is the vacuum permittivity, and the brackets indicate that all quantities are to be evaluated at the retarded time

$$\tau = t - R(\tau)/c. \tag{3.2}$$

[2]Note that a uniform distribution of length l has a standard deviation $\sigma_z = l/\sqrt{12}$.

2021 JINST 16 P10010

The magnetic field is given by $\mathbf{B} = \mathbf{n} \times \mathbf{E}/c$ [18]. The velocity term is sometimes called the "space charge" or "Coulomb" term because of the $1/R^2$ scaling, while the acceleration term is sometimes called the "radiation" term because of the $1/R$ scaling.

In an alternative formulation, for given charge and current densities $\rho(\mathbf{x}, t)$ and $\mathbf{J}(\mathbf{x}, t)$ at position $\mathbf{x}$ and time t, the electric field $\mathbf{E}(\mathbf{x}, t)$ can be calculated using Jefimenko's form of Maxwell's equations:

$$\mathbf{E}(\mathbf{x}, t) = \frac{1}{4\pi\epsilon_0} \int d^3x' \left[\frac{\mathbf{R}}{R^3} \rho(\mathbf{x}', \tau) + \frac{\mathbf{R}}{c\, R^2} \dot{\rho}(\mathbf{x}', \tau) - \frac{1}{c^2\, R} \dot{\mathbf{J}}(\mathbf{x}', \tau) \right]_{\tau = t - R/c}, \tag{3.3}$$

in which $\mathbf{R} \equiv \mathbf{x} - \mathbf{x}'$, $R \equiv \|\mathbf{R}\|$ [18]. In this formulation, the retarded points $\mathbf{x}'$ and times t' are independent variables, so there are no functions that need to be inverted. Therefore, if one knows ρ, $\dot{\rho}$, and $\dot{\mathbf{J}}$ at all points in space $\mathbf{x}'$ and for all times $t' \leq t$, with a dot denoting the time derivative, then this formula gives the electric field by direct integration.

These formulations are amenable to analytic calculations for particles moving on fixed geometries. The total field is then the sum of the fields for each particle. While this approach is best suited for calculations in free space, the effect of shielding can be straightforwardly included for planar motion by using an infinite array of image charges.

Another approach is to solve Maxwell's equations directly for a charged particle in a conducting beam chamber. This is necessary for situations with strong shielding. While this is difficult in general, analytic solutions can be found by making assumptions about the beam chamber geometry (e.g., cylindrical pill box, toroidal) and conductivity, as well as the current source (on-axis, constant velocity). Such systems were first studied by Neil at al. in the 1960s [27, 28]. Warnock and Morton [29], Ng [30] and Karliner et al. [31] independently studied the resonance modes and resistive wall effects in 1988. Reference [29] concludes that wave numbers less than $h\sqrt{\rho/w}$ should be suppressed for a chamber width w. An alternative approach to calculate fields in the frequency domain was introduced in 2003 by Stupakov & Kotelnikov [32].

3.2 One-dimensional analytic models

One-dimensional models are important because they give insight into the overall structure and scaling of the problem and can motivate the development of higher dimensional models.

Equation 3.1 can be simplified if we consider charges that move on the same trajectory at the same speed, but distributed in time. This is called the line charge model. For motion on a circle, the 1D CSR wakefield was first derived in 1960 by Iogansen & Rabinovich [33]. Murphy et al. used a similar method to include the effect of shielding by parallel plates in 1996 [34].

These earlier developments focused on purely circular geometries, but practically all modern accelerators are composed of separated magnets. The need to calculate the transient effects in bunch-compression systems led Saldin et al., in 1997, to develop an ultra-relativistic 1D model of the longitudinal CSR wakefield in an isolated bending magnet. Using small-angle approximations they derive the 1D longitudinal CSR wakefield for a bunch entering a bend as

$$\begin{aligned} W_s(z) &= -\frac{2}{3^{1/3}} \frac{N r_c m c^2}{\rho^{2/3}} \left[\frac{\lambda(z - z_L) - \lambda(z - 4z_L)}{z_L^{1/3}} + \int_{z - z_L}^{z} \frac{1}{(z - z')^{1/3}} \frac{\partial \lambda(z')}{\partial z'}\, dz' \right], \\ z_L &\equiv \frac{\rho\, \phi^3}{24}, \end{aligned} \tag{3.4}$$

where $\lambda(z)$ is the normalized longitudinal bunch density at $z = s - \beta ct$, z_L is called the slippage length, and ϕ is the angle traveled into the magnet by the bunch center [35]. If the extent of λ is greater than the slippage length then the first terms are zero, and this is called the steady-state wakefield. Otherwise this is called the entrance transient wakefield. Note that this formula only accounts for the acceleration term in eq. (3.1).

Reference [35] also establishes four basic geometrical cases to consider for a source particle P' that travels behind observation particle P on the same trajectory:

Case A P' traveling on a straight line, P inside a following bend (entering).

Case B Both particles within a bend (steady-state).

Case C P' and P traveling on straight lines before and after a bend, respectively (straddling).

Case D P' within a bend, P inside the straight line following a bend (exiting).

These were further clarified by Stupakov & Emma [36] in 2002. Many years later, motivated by the need to study CSR in FFA magnets in CBETA [37], Lou & Hoffstaetter extended these for cases (**E**, **F**, **G**, **H**, and sub-cases) that consider two bending magnets [38]. The total wakefield of a bunch is obtained by integrating the bunch density over formulas for the appropriate cases.

One-dimensional longitudinal models similar to eq. (3.4) have been extensively studied and developed over subsequent decades. In 2009 Sagan et al. extended the formalism to include systems of arbitrary bends and drifts, with a non-singular form of the integrand and finite energy [39]. In the same year Mayes & Hoffstaetter removed all relativistic and small-angle approximations and developed an exact formalism using the Jefimenko equations (eq. (3.3)), including shielding by parallel plates [24]. This method was used to validate the range of applicability of ref. [39].

One-dimensional models for the transverse force have been controversial. In 1985 Talman examined the transverse force from eq. (3.1) for a thin line charge, and remarked that it has a logarithmic singularity for zero transverse size [3]. This is called the Centrifugal Space Charge Term (CSCF).[3] At the time this was thought to have serious consequences for electron storage rings, which prompted a workshop in the same year and many studies [40]. Lee studied this in 1990 and argued that this force is nearly canceled by the change in potential energy of the beam in a bend [41]. In 1996 Derbenev & Shiltsev [42] rederived the CSCF and showed that a thin bunched beam has a "centrifugal" transverse wakefield

$$W_x^{(1)}(z) = N r_c m c^2 \frac{\Lambda}{\rho} \lambda(z), \tag{3.5}$$

where $\Lambda = \log\left[(\rho\sigma_z^2/\sigma_x^3)^{2/3}(1+\sigma_x/\sigma_z)\right]$, and σ_x is the horizontal size of the bunch. However, like Lee they concluded that this does not contribute to the beam dynamics, and instead they introduce a "centripetal" transverse wakefield

$$W_x^{(2)}(z) = -N r_c m c^2 \frac{2}{\rho} \lambda(z), \tag{3.6}$$

which has the opposite sign and no dependence on the transverse beam size. The subject has been the source of many animated papers and discussions [43, 44].

[3]This is also known colloquially as the "Talman force".

The simplicity of 1D line-charge models comes at a cost, as the electric field within an infinitesimally thin line-charge is infinite. All derivations of 1D wakefields using line-charge models must use some sort of regularization scheme, such as subtracting off a Coulomb-like term, in order to obtain finite values [45]. This is often justified by the fact that averaging W_s over the bunch distribution recovers the correct coherent power loss.[4] However this is not theoretically satisfying, and it has led to confusion about how to analyze these models. Extending the charge distributions to two- and three-dimensions alleviates this problem.

3.3 Two- and three-dimensional analytic models

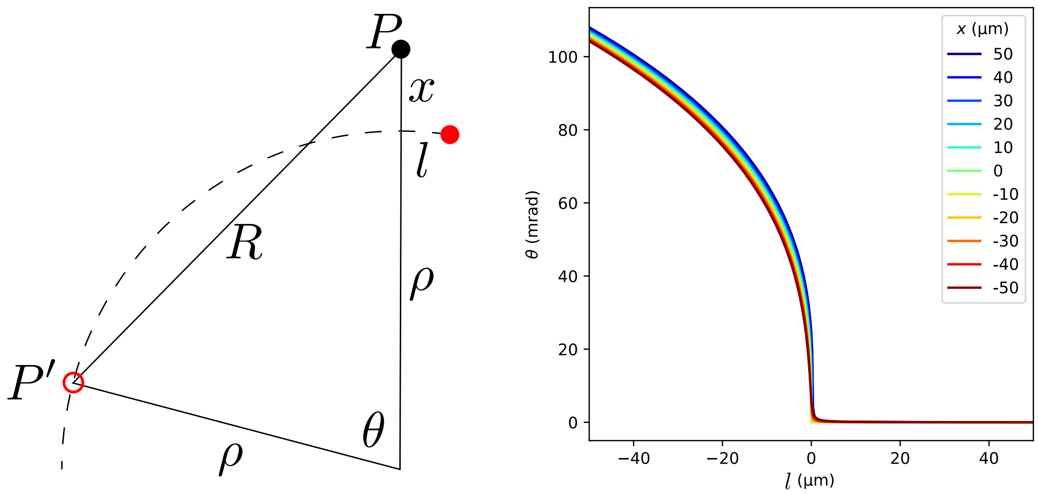

(a) Retarded geometry **(b)** Retarded angle

Figure 1. (a) Basic CSR geometry for a source particle in position P' at the retarded time t', influencing an observation particle at position P at the current time t. The solid red dot is the source particle also at the current time t, which has a local arc length difference l from the observation particle. (b) The retarded angle θ in this geometry for various l and x with $\gamma = 500$ and $\rho = 1$ m.

In principle it is straightforward to develop 2D and 3D models for CSR by using eq. (3.1) with prescribed trajectories, such as motion on a circle. Figure 1 shows such a geometry, and using the definition of retarded time in eq. (3.2) we can write the longitudinal distance l from the source to observation particle (at the current time t) as

$$\frac{l}{\rho} = \theta - \beta\sqrt{\left(\frac{x}{\rho}\right)^2 + \left(\frac{y}{\rho}\right)^2 + 4\left(1 + \frac{x}{\rho}\right)\sin^2\left(\frac{\theta}{2}\right)}, \tag{3.7}$$

where θ is the retarded angle of the source particle and y is up, out of the page. This and eq. (3.1) allow us to calculate the fields given particle positions at the current time t. Figure 2 illustrates how distorted a regular pattern of particles can look in their retarded positions. Defining $z = s - \beta ct$ with s as the arc length also gives $l = z' - z$, where the prime denotes the values at the retarded time.

[4] Indeed, averaging the steady-state term in eq. (3.4) over a Gaussian bunch distribution will recover eq. (2.8) exactly.

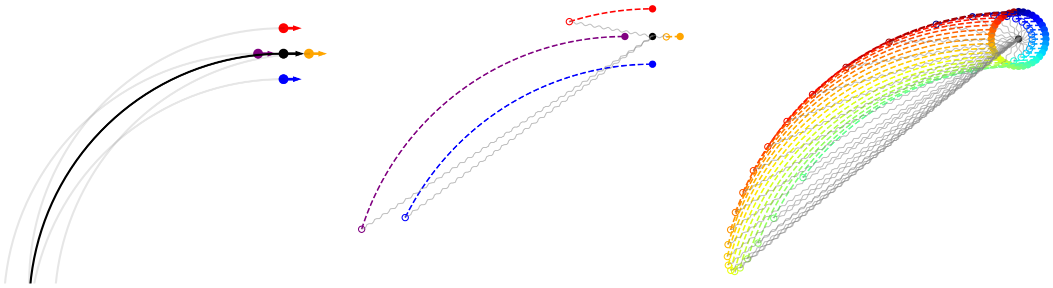

(a) Circular trajectories **(b)** 4 retarded sources **(c)** 36 retarded sources

Figure 2. Visualization of retarded positions in two dimensions for particles in circular motion. In (a) an observation particle (black) is surrounded by four particles (solid dots) at the same observation time. In (b) the retarded positions for these particles are shown as circles, from which a photon can be emitted that reaches the observation particle. By the retardation condition, the time for each photon to do this is the same as the time elapsed as these particles traverse the dashed line. (c) shows the same, but with 36 particles.

Equation 3.7 is a transcendental equation in θ with no known closed-form solutions, so approximations are often used to invert it. For example, with $x = 0$, $y = 0$, and assuming positive l, eq. (3.7) can be expanded as

$$\frac{l}{\rho} = \theta - 2\beta \sin\left(\frac{\theta}{2}\right) \tag{3.8}$$

$$\simeq (1-\beta)\theta + \frac{\beta\theta^3}{24} + O\left(\theta^5\right), \tag{3.9}$$

which is a depressed cubic equation and therefore has an analytic solution. This is also the definition of the slippage length in eq. (3.4) with $\beta \to 1$. Similarly the full eq. (3.7) can be expanded into a depressed quartic equation, which also has a known analytic solution. In 2013 Huang et al. [6] pioneered several such expansions in two dimensions, including a Padé approximatant, and developed a two-dimensional model for the longitudinal CSR wakefield including the entrance transient case.

A significant advance occurred in 2017 when Cai developed a 2D steady-state model without approximations in the retarded angle or energy [7], and then in 2020 a full 3D steady-state model [8]. In 2021 he continued the work in 2D to include the four transient cases **A**–**D** described in section 3.2. One of the essential aspects is to simply leave eq. (3.7) in the formulas without approximation, to be numerically evaluated later. Formulas for the transverse, vertical, and longitudinal electric fields E_x, E_y, E_s and magnetic fields B_x, B_y, B_s are then easily written. With the paraxial approximation ($\beta_x \approx 0$, $\beta_y \approx 0$, $\beta_s \approx \beta$), the transverse forces F_x and F_y are also easily written.

For example, the longitudinal electric field in eq. (3.1) is

$$E_s(\chi,\zeta,\xi) = \frac{q}{4\pi\epsilon_0}\frac{\beta^2}{\rho^2}\frac{(\sin\theta - \beta\kappa\cos\theta)/(\beta\gamma)^2 + [\cos\theta - (1+\chi)]\,[(1+\chi)\sin\theta - \beta\kappa] - \zeta^2\sin\theta}{[\kappa - \beta(1+\chi)\sin\theta]^3}, \tag{3.10}$$

where $\kappa \equiv R/\rho = \sqrt{\chi^2 + \zeta^2 + 4(1+\chi)\sin^2\frac{\theta}{2}}$, and we use the convenient notation $\chi \equiv x/\rho$, $\zeta \equiv y/\rho$, as in ref. [8]. Further defining $\xi = -l/2\rho = (z' - z)/2\rho$, the longitudinal 3D steady-state

2021 JINST 16 P10010

CSR wakefield due to a normalized bunch distribution λ with charge $Q = Nq$ is then given by the convolution over the electric field

$$W_s(x, y, z) = \iiint E_s\left(\frac{x - x'}{\rho}, \frac{y - y'}{\rho}, \frac{z - z'}{2\rho}\right) Q\lambda(x', y', z') dx'dy'dz'. \tag{3.11}$$

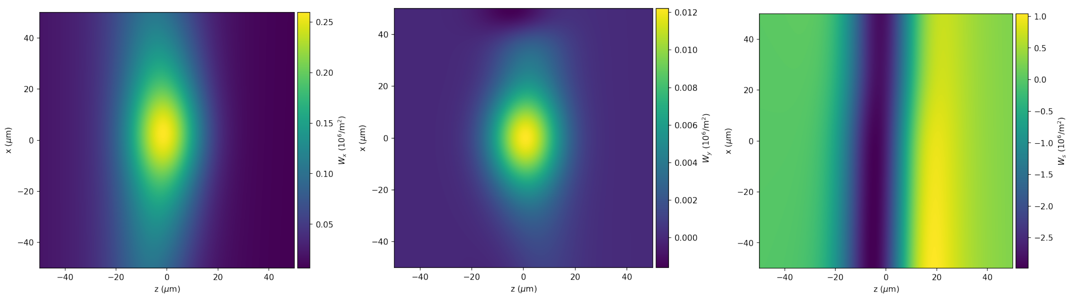

(a) Horizontal wakefield at $y = 0$ **(b)** Vertical wakefield at $y = \sigma_y$ **(c)** Longitudinal wakefield at $y = 0$

Figure 3. Visualization of the total 3D steady-state CSR wakefield from ref. [8]. This uses the PyCSR3D package with parameter set A in table 1. The horizontal and vertical wakes use the integrated Green function method described in section 4.3 on the Lorentz force directly, while the longitudinal wake uses the potential function described in this section. Note that these plots are in units normalized by $Nr_c mc^2$.

However, the force formulas are difficult to use numerically because of a strong coordinate singularity at the origin. One solution is to find "potential" functions for the fields and forces, so that $E_s \propto \partial w_s/\partial \xi$, and then to integrate by parts to obtain

$$W_s(x, y, z) = Nr_c mc^2 \iiint w_s\left(\frac{x - x'}{\rho}, \frac{y - y'}{\rho}, \frac{z - z'}{2\rho}\right) \frac{\partial \lambda(\chi', \zeta', z')}{\partial z'} dx'dy'dz', \tag{3.12}$$

where the potential (kernel) function is

$$w_s(\chi, \zeta, \xi) = \frac{\beta^2}{\rho} \frac{\cos\theta - \frac{1}{1+\chi} - \frac{1}{\beta^2\gamma^2}}{\kappa - \beta(1 + \chi)\sin\theta}. \tag{3.13}$$

A different approach, suitable for when integration by parts is not practical, is to use the integrated Green function method as described in section 4.3. The transient forms of these results are similar, but with finite integration limits and multiple terms. Nevertheless, they are of a form that can be readily evaluated and integrated numerically. Figure 3 shows the total 3D wakefields due to a simple Gaussian beam, with parameters defined in table 1. Note that these plots are shown in units normalized by $Nr_c mc^2$.

Table 1. Test parameter sets for illustrating the CSR wake. These use uncorrelated Gaussian distributions with standard deviations $\sigma_x, \sigma_y, \sigma_z$. The instantaneous velocity is in the z direction.

Name	σ_x (μm)	σ_y (μm)	σ_z (μm)	ρ (m)	γ
A	10	10	10	1	500
B	10	1	10	1	500

For arbitrary trajectories, Stupakov & Tang in 2021 developed an approach to calculate the fields using forms very similar to eq. (3.3), with the current density expressed as the product of the charge density and the local velocity, and the time derivative of the charge density eliminated using the continuity equation [10]. They adapt the formulas in 2D using Frenet-Serret curvilinear coordinates, which can then be evaluated numerically. Besides the arbitrary trajectories, this method has the advantage of being able to capture the effects of a compressing bunch due to energy deviations. The cost, however, is that the history of the charge and current densities must be known in advance.

4 Numerical computation

Most complex accelerator effects cannot be calculated from a formula and must be evaluated using numerical simulations. Accelerator simulations have been performed at least since the 1960s [46]. The need to accurately estimate the emittance growth due to CSR in bunch compressors in FELs drove the development of many simulation codes, some specialized and some general purpose.

4.1 One-dimensional numerical approaches

One-dimensional models are most commonly used in complex simulations because of their speed. The simplicity of eq. (3.4) allowed Borland to develop it into an algorithm for ELEGANT in 2001 [47], which is still used and relied upon today. Like many accelerator codes, ELEGANT has the concept of discrete elements (e.g., bending magnets, drifts) that form the basic reference geometry to use in the calculation, and therefore the basic cases described above can be implemented.

In 2009 Sagan et al. incorporated the formalism in ref. [39] for arbitrary bends and drifts into BMAD[48] by slicing the bunch and incorporating the space charge effect using an approximate formula for the force from a thin Gaussian slice. Later in 2017 Sagan & Mayes realized that a general approximation given by Saldin et al. in 1998 [49] could be implemented in BMAD, which simplified and extended the calculation to arbitrary off-axis trajectories by recording the history of the bunch trajectory and using a spline fit to locate the retarded positions via numerical root finding [50]. In 2018 Brynes et al. described a similar method, used in the code GPT [51], that makes use of off-axis sample particles in the slices and their histories to compute the full fields from eq. (3.1) [52].

4.2 Field-based numerical approaches

The effect of shielding in some of these codes is mimicked using image charges. This however only works for movement in one plane (e.g., the horizontal plane, using vertical image charges). The end of section 3.1 describes approaches for solving Maxwell's equations in pure goemetries, but different approaches are needed to simulate complex chamber geometries or transient effects. One of the first to do this for CSR was Agoh & Yokoya, who developed an approach in 2004 to propagate fields on a computational mesh in the frequency domain, with the equations simplified by using the paraxial approximation and a fixed line-charge distribution. They developed a custom code that was later used to verify the parallel-plate method in BMAD [39]. An excellent summary of this and previous approaches was also written by Agoh in ref. [53].

2021 JINST 16 P10010

More recently in 2016 Warnock & Bizzozero expanded on these methods to extend the charge distribution in the vertical direction and allow for complex wall chambers. In the time domain, Novokhatski describes an implicit scheme to solve for the fields on a traveling mesh [54]. In 2019 Bizzozero et al. developed a code that used a high-order discontinuous Galerkin method to compute CSR in a complicated bunch compressor chamber [55].

4.3 Two-dimensional particle-based numerical approaches

Two-dimensional CSR wakefields were actually studied numerically as early as 1997 by Dohlus & Limberg by slicing the bunch transversely and calculating the fields due to many 1D bunches [56]. This eventually evolved into CSRTRACK, which is still used today to explore 2D effects [57]. One of the methods in CSRTRACK is to track "sub-bunches" that have a fixed Gaussian shape, and to track these backwards in time to find the retarded positions. Formulas derived from the retarded potentials are integrated over each sub-bunch to obtain the field on a 2D mesh in the horizontal plane. This does not consider vertical forces [58, 59].

Capturing the effect of the microbunching instability can be challenging for bunch compressor systems, so in 2009 Bassi et al. developed a 2D Vlasov-Maxwell approach, which naturally includes CSR, to explore this self-consistently [60]. The corresponding 2D CSR code is now named VM3@A (Vlasov-Maxwell Monte-Carlo Method at Albuquerque) [61]. For each tracking step, particles are converted to a smooth representation using a Fourier method, where the Fourier coefficients are calculated via a Monte-Carlo integration. This permits the accurate and efficient storage over a "history" of the charge density and its spatial and time derivatives, allowing for the calculation of the electromagnetic fields via a two-dimensional integration that accounts for retardation effects.

Starting in 2020, Lou et al. have been developing an efficient convolutional approach to evaluate the 2D wakefield formulas by Cai as described in section 3.3. The goal is to prototype the numerical methods so that they can be incorporated into a general purpose beam dynamics code such as BMAD. To this end they are developing the open-source PYCSR2D Python package [11, 62].

The unique feature of these wakefield formulas is that is they are written as a convolution. For example, in one dimension, consider

$$W(z) = \int G(z - z')\lambda(z')\, \mathrm{d}z', \tag{4.1}$$

where λ is a bounded distribution. A simple and robust way to solve this is to discretize the system. Let the values of z be restricted to a set $\{z_k\}$, and denote $\lambda_k = \lambda(z_k)$, $W_k = W(z_k)$. If the values z_k are also chosen to be on a regular grid, so that $z_k = k\Delta$ for some grid spacing Δ, and if λ is approximated to be constant over each interval Δ, then we have

$$\begin{align}
W_k &= \int G(z_k - z')\lambda(z')\, \mathrm{d}z' \tag{4.2}\\
&\approx \sum_{k'} \lambda_{k'} \underbrace{\int_{z_k - z'_k - \Delta/2}^{z_k - z'_k + \Delta/2} G(z'')\, \mathrm{d}z''}_{\overline{G}(z_k - z_{k'}) \equiv \overline{G}_{k-k'}} \tag{4.3}\\
&= \sum_{k'} \lambda_{k'} \overline{G}_{k-k'}, \tag{4.4}
\end{align}$$

which is now in the form of a discrete convolution. The function $\overline{G}$ is simply the integral of G over a grid cell. This is known as the integrated Green function (IGF) method and has been used for some time now in space charge calculations, because the indefinite integral can be performed analytically [63, 64]. Discrete convolutions of this form can be evaluated very efficiently in parallel using Fast Fourier Transform (FFT) method, as described in ref. [65].

PyCSR2D takes particle x and z positions as inputs and deposits them on an $n_x \times n_z$ grid using a cloud-in-cell algorithm. After some smoothing, the partial derivative in the z direction is computed using finite differences. It then constructs a $2n_x \times 2n_z$ (double-sized) grid of spatial coordinates, with the origin at the center, and evaluates the integrated Green function on this grid based on one of the kernel functions. The choice of the kernel depends on the geometry, such as using eq. (3.13) at $y = 0$ for a bunch that is well inside a bend. Convolving the two grids produces the total wakefield on an $n_x \times n_z$ grid that is aligned with the initial distribution. Values at the original particle positions are then found using interpolation.

4.4 Three-dimensional particle-based numerical approaches

Computing CSR in three dimensions has only been pursued recently because of the seemingly high computational cost. In order to evaluate the validity of simplified models and explore single-particle effects, Ryne et al. in 2012 developed a large-scale parallel program to calculate the field directly from the full number of particles in a bunch using eq. (3.1) [66]. They tested this on up to 6.24 billion particles (equivalent to 1 nC of electrons). By gathering statistics on many realizations with different random seeds, they observed that the fluctuations in the field in the center of the bunch grow as γ^2. The initial code was not self-consistent, in that the forces calculated did not act back on the particles.

This evolved into the self-consistent N-body LW3D code that is currently being developed by Ryne [67]. At each timestep, for an observation point, the history of each particle is used to find the retarded position and evaluate the field using eq. (3.1). For self-consistent calculations, the observation points can be on a grid to be interpolated, or at the position of each particle for precise forces. To benchmark the code, Ryne compares against an analytical model solved by Synge in 1940 for the time for two charged particles to collide [68].

LW3D is naturally able to compute the CSR wakefield. To illustrate this, we use a highly simplified case of a spherically symmetric Gaussian bunch in which, at an instant, each particle has the same velocity in the z direction. Table 1 shows the parameters. The particles are tracked in an external, vertical magnetic field, without interactions, on a complete circle to record their histories. Figure 4 shows the resultant fields on lines across the bunch, illustrating the stochastic effects.

In a different approach, Huang is developing the open-source code CoSyR that uses eq. (3.1) to create wavefronts for each particle along the bunch trajectory. These wavefront meshes and associated Liénard-Wiechert fields and potentials are combined onto a common grid, which is then used to calculate the beam field for each timestep. The code takes advantage of modern high performance computing architectures using GPUs and can handle the self-consistent beam dynamics from non-steady-state CSR wakes. Currently it is best suited for low energy beams.

Finally, Mayes is developing the open-source PyCSR3D Python package [69] and a companion OpenCSR Fortran library [70] that expand on the developments in PyCSR2D to implement the 3D convolutional formulas developed by Cai. The concept is the same as that described for PyCSR2D,

2021 JINST 16 P10010

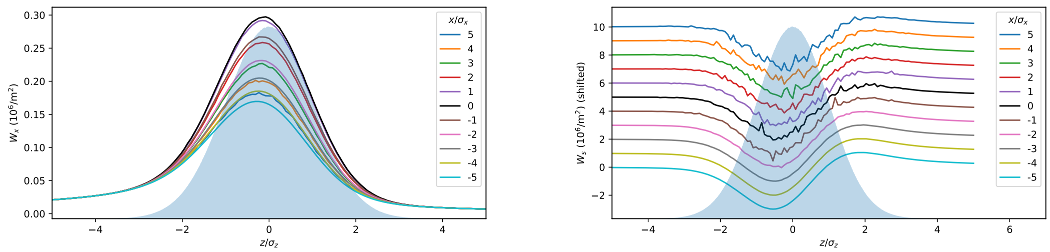

(a) Horizontal wakefield **(b)** Longitudinal wake

Figure 4. Horizontal and longitudinal CSR wakes in $y = 0$ plane calculated by LW3D using 625 million particles (equivalent to 100 pC of electrons) according to parameter set A in table 1. The longitudinal wakes have been offset in the graph for clarity. Even with this many particles, stochastic effects can be seen.

but on an $n_x \times n_y \times n_z$ grid. OpenCSR is parallelized with OpenMP and uses FFTW [71] for the convolutional step, which enables the algorithm to run in seconds on a personal computer for modest grid parameters. It is incorporated in Bmad as a dependency. Figure 5 shows the field along lines in the z direction, with a comparison to 1D models.

Figure 6 offers a comparison of the total CSR wakefield computed by some of these methods for the simple test parameters in table 1. Here we consider LW3D to be the reference method, because it simulates every electron in the beam without smoothing. The longitudinal wakes agree well between all methods, even though LW3D predicts highly stochastic behavior (which cannot be captured easily with existing meshing methods). The transverse wakes exhibit the same general behaviour, with noticeable differences between the 2D and 3D methods that show the importance of the full 3D calculation. Overall, the horizontal wake for all methods is positive and tends to agree with the CSCF in eq. (3.5).

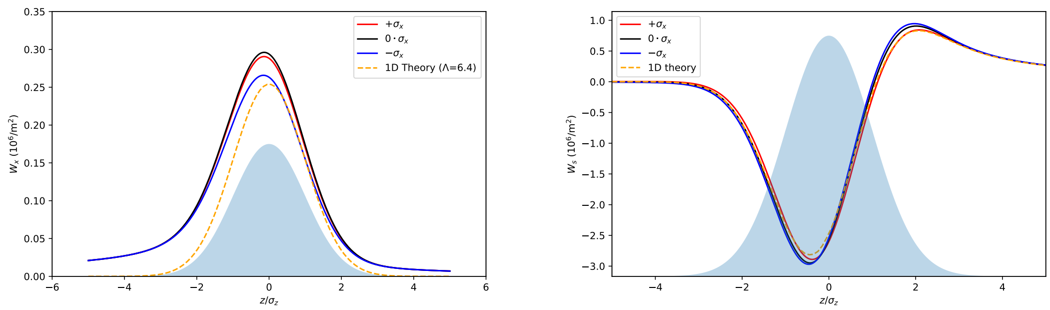

(a) Horizontal wakefield **(b)** Longitudinal wake

Figure 5. Horizontal and longitudinal wakes in the $y = 0$ plane, calculated by PyCSR3D using parameter set A in table 1. These are essentialy lines taken across Figure 3. In (a), the 1D theory is taken as eq. (3.5), whereas in (b) the 1D theory is the steady-state term in eq. (3.4).

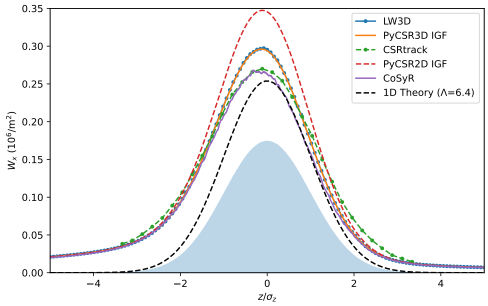

(a) Horizontal wake at $x = 0$, $y = 0$, parameter set A

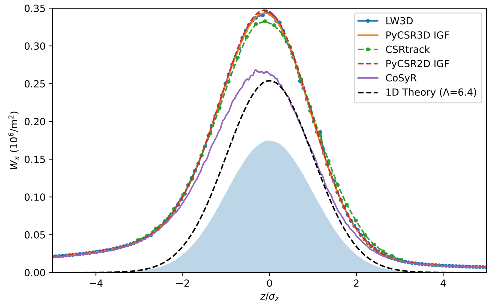

(b) Horizontal wake at $x = 0$, $y = 0$, parameter set B

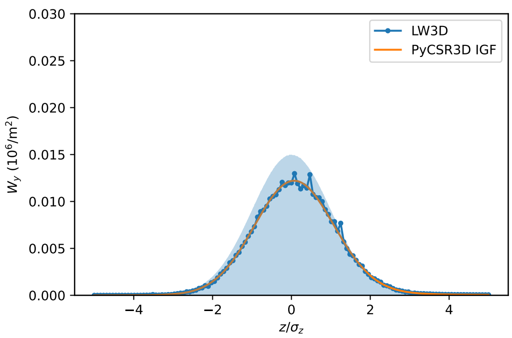

(c) Vertical wake at $x = 0$, $y = \sigma_y$, parameter set A

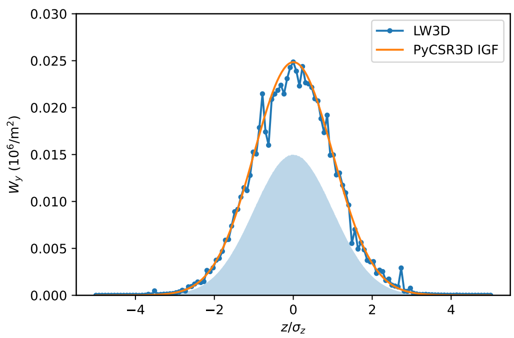

(d) Vertical wake at $x = 0$, $y = \sigma_y$, parameter set B

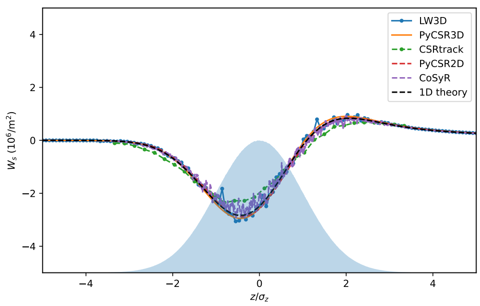

(e) Longitudinal wake at $x = 0$, $y = 0$, parameter set A

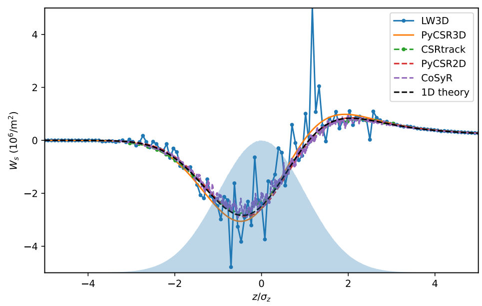

(f) Longitudinal wake at $x = 0$, $y = 0$, parameter set B

Figure 6. Comparison of the total CSR wakefield along the z axis according to the parameters in table 1 for various codes. LW3D is shown using 624 million particles and exhibits highly stochastic behavior in the longitudinal wake that is not easily captured by the other mesh-based methods. PyCSR3D uses an integrated Green function (IGF) approach over the transverse forces for the horizontal and vertical wakes and uses the potential form from eq. (3.13) for the longitudinal wake. CSRtrack is shown using 100k particles. CoSyR is shown using 300k particles in its 2D mode with smoothing and only considers the acceleration term in eq. (3.1). Parameter set A is a spherically symmetric Gaussian beam, while parameter set B has a vertical size that is smaller by a factor of 10. CoSyR and PyCSR2D only consider forces in the $y = 0$ plane and are therefore the same in both parameter sets. Only LW3D and PyCSR3D are able to produce the vertical wakes and, besides the stochastic effects, show excellent agreement in all of these examples.

2021 JINST 16 P10010

5 Outlook

Computing CSR in detail within a bunch, especially in three dimensions, is one of the most challenging problems in accelerator physics. In the past a great deal of effort was spent on making approximations and reducing the dimensionality of the problem. In recent years we have been able to remove these assumptions and directly use the equations that were developed more than a century ago.

This is possible not only because of the availability of modern parallel computing resources, but also because of the many layers of software abstraction available to the researcher. To go forward, the community will increasingly need to rely on open and collaborative software development practices. Some of the codes mentioned in this paper are open source or being moved toward it, but many cited in the literature remain closed off or abandoned [72]. All of the approaches shown have limitations, bugs, and inefficiencies, and addressing these will be expedited by better collaboration.

The developments toward modeling full 3D CSR are just beginning. As we continue toward routinely simulating every particle in a bunch, we will start to probe the limitations of classical electrodynamics. Controversial topics such as radiation reaction may need to be revisited, as well as the degree to which we can think of simulated point charges as real [73].

Acknowledgments

We would like to think G. Bassi, Y. Cai, M. Dohlus, C. Huang, W. Lou, A. Novokhatski, R. Ryne, R. Talman, J. Tang, N. Taylor, R. Warnock, G. White for useful discussions and materials regarding this manuscript. This research used resources of the National Energy Research Scientific Computing Center (NERSC), a U.S. Department of Energy Office of Science User Facility located at Lawrence Berkeley National Laboratory, operated under Contract No. DE-AC02-05CH11231.

References

[1] J.B. Murphy, *An introduction to coherent synchrotron radiation in storage rings*, *ICFA Beam Dynamics Newsletter #35* (2004) 20.

[2] K.L.F. Bane et al., *Measurements and Modeling of Coherent Synchrotron Radiation and its Impact on the LCLS Electron Beam*, *Phys. Rev. ST Accel. Beams* **12** (2009) 030704.

[3] R. Talman, *Novel Relativistic Effect Important in Accelerators*, *Phys. Rev. Lett.* **56** (1986) 1429.

[4] V. Yakimenko et al., *Prospect of Studying Nonperturbative QED with Beam-Beam Collisions*, *Phys. Rev. Lett.* **122** (2019) 190404 [arXiv:1807.09271].

[5] V. Yakimenko et al., *FACET-II facility for advanced accelerator experimental tests*, *Phys. Rev. Accel. Beams* **22** (2019) 101301.

[6] C. Huang, T.J.T. Kwan and B.E. Carlsten, *Two dimensional model for coherent synchrotron radiation*, *Phys. Rev. ST Accel. Beams* **16** (2013) 010701.

[7] Y. Cai, *Coherent synchrotron radiation by electrons moving on circular orbits*, *Phys. Rev. Accel. Beams* **20** (2017) 064402.

[8] Y. Cai and Y. Ding, *Three-dimensional effects of coherent synchrotron radiation by electrons in a bunch compreSSOR*, *Phys. Rev. Accel. Beams* **23** (2020) 014402.

[9] Y. Cai, *Two-dimensional theory of coherent synchrotron radiation with transient effects*, *Phys. Rev. Accel. Beams* **24** (2021) 064402.

[10] G. Stupakov and J. Tang, *Calculation of the wake due to radiation and space charge forces in relativistic beams*, *Phys. Rev. Accel. Beams* **24** (2021) 020701.

[11] W. Lou, C. Mayes, Y. Cai and G. White, *Simulating two dimensional coherent synchrotron radiation in python*, in *Proceedings of 12^th International Particle Accelerator Conference*, Campinas, Brazil, 24–28 May 2021, WEPAB234.

[12] J. Larmor, *LXIII. On the theory of the magnetic influence on spectra; and on the radiation from moving ions*, *London Edinburgh Dublin Philos. Mag. J. Sci.* **44** (1897) 503.

[13] A. Liénard, *Champ électrique et magnétique produit par une charge électrique concentrée en un point et animée d'un mouvement quelconque*, *L'Éclairage Électrique* **XVI** (1898) 5.

[14] D. Iwanenko and I. Pomeranchuk, *On the Maximal Energy Attainable in a Betatron*, *Phys. Rev.* **65** (1944) 343.

[15] J.P. Blewett, *Radiation Losses in the Induction Electron Accelerator*, *Phys. Rev.* **69** (1946) 87.

[16] G. Schott, *Electromagnetic Radiation*, Cambridge (1912).

[17] J. Schwinger, *On radiation by electrons in a betatron*, 1945, https://doi.org/10.2172/1195620.

[18] J.D. Jackson, *Classical electrodynamics*, 3rd edition, Wiley, New York, NY, U.S.A. (1999).

[19] H.C. Pollock, *The discovery of synchrotron radiation*, *Am. J. Phys.* **51** (1983) 278.

[20] G. Parzen, *The radiation from an electron moving in a uniform magnetic field*, *Phys. Rev.* **84** (1951) 235.

[21] D.R. Corson, *Radiation by electrons in large orbits*, *Phys. Rev.* **90** (1953) 748.

[22] D.H. Tomboulian and P.L. Hartman, *Spectral and Angular Distribution of Ultraviolet Radiation from the 300-Mev Cornell Synchrotron*, *Phys. Rev.* **102** (1956) 1423.

[23] J.S. Schwinger, *On the classical radiation of accelerated electrons*, *Phys. Rev.* **75** (1949) 1912.

[24] C. Mayes and G. Hoffstaetter, *Exact* $1-D$ *Model for Coherent Synchrotron Radiation with Shielding and Bunch Compression*, *Phys. Rev. ST Accel. Beams* **12** (2009) 024401 [arXiv:0812.3189].

[25] C. Mayes, *Energy Recovery Linear Accelerator Lattice Design and Coherent Synchrotron Radiation*, dissertation, Cornell University, Ithaca, NY, U.S.A. (2009).

[26] J.S. Nodvick and D.S. Saxon, *Suppression of Coherent Radiation by Electrons in a Synchrotron*, *Phys. Rev.* **96** (1954) 180.

[27] V.K. Neil, *A study of some coherent electromagnetic effects in high-current particle accelerators*, Ph.D. thesis, University of California, Berkeley, CA, U.S.A. (1960).

[28] V.K. Neil, D.L. Judd and L.J. Laslett, *Coherent electromagnetic effects in high current particle accelerators: II. Electromagnetic fields and resistive losses*, *Rev. Sci. Instrum.* **32** (1961) 267.

[29] R.L. Warnock and P.L. Morton, *Fields Excited by a Beam in a Smooth Toroidal Chamber: Pt. 1. Longitudinal Coupling Impedance*, *Part. Accel.* **25** (1990) 113.

[30] K.-Y. Ng, *Resonant Impedance in a Toroidal Beam Pipe*, *Part. Accel.* **25** (1990) 153.

[31] M.M. Karliner, N.V. Mityanina and V.P. Yakovlev, *The impedance of a toroidal chamber with walls of finite conductivity. waveguide model.*, Tech. Rep., BUDKERINP 93-90, Budker Institute of Nuclear Physics, Novosibirsk, Russia (1993).

2021 JINST 16 P10010

[32] G.V. Stupakov and I.A. Kotelnikov, *Shielding and synchrotron radiation in toroidal waveguide*, *Phys. Rev. ST Accel. Beams* **6** (2003) 034401.

[33] L.V. Iogansen and M.S. Rabinovich, *Coherent electron radiation in the synchrotron II*, *Sov. Phys. JETP* **37** (1960) 83.

[34] J.B. Murphy, S. Krinsky and R.L. Gluckstern, *Longitudinal wake field for an electron moving on a circular orbit*, *Part. Accel.* **57** (1997) 9.

[35] E.L. Saldin, E.A. Schneidmiller and M.V. Yurkov, *On the coherent radiation of an electron bunch moving in an arc of a circle*, *Nucl. Instrum. Meth. A* **398** (1997) 373.

[36] G. Stupakov and P. Emma, *CSR wake for a short magnet in ultrarelativistic limit*, in *Proceedings of 8th European Particle Accelerator Conference*, Paris, France, 3–7 June 2002, pp. 1479–1481.

[37] G.H. Hoffstaetter et al., *CBETA Design Report, Cornell-BNL ERL Test Accelerator*, arXiv:1706.04245.

[38] W. Lou and G. Hoffstaetter, *Coherent synchrotron radiation wake expressions with two bending magnets and simulation results for a multiturn energy-recovery linac*, *Phys. Rev. Accel. Beams* **23** (2020) 054404 [arXiv:2001.06960].

[39] D.C. Sagan, G.H. Hoffstaetter, C.E. Mayes and U. Sae-Ueng, *Extended 1D Method for Coherent Synchrotron Radiation including Shielding*, *Phys. Rev. ST Accel. Beams* **12** (2009) 040703 [arXiv:0806.2893].

[40] E. Keil, *Notes on the first workshop on radiation impedance*, Tech. Rep., CERN-LEP-TH-85-40, CERN, Geneva, Switzerland (1985).

[41] E.P. Lee, *Cancellation of the centrifugal space charge force*, *Part. Accel.* **25** (1990) 241.

[42] Y.S. Derbenev and V.D. Shiltsev, *Transverse effects of microbunch radiative interaction*, Tech. Rep., SLAC-PUB-7181, FERMILAB-TM-1974 (1996).

[43] G. Geloni, E. Saldin, E. Schneidmiller and M. Yurkov, *Misconceptions regarding the cancellation of selfforces in the transverse equation of motion for an electron in a bunch*, physics/0310133.

[44] R. Li and Y.S. Derbenev, *Discussions on the Cancellation Effect on a Circular Orbit*, *Conf. Proc. C* **0505161** (2005) 1631.

[45] K. Heinemann, G. Bassi and J. Ellison, *Comparison of three CSR radiation powers for particle bunches and line charges*, in *Proceedings of the 10th European Particle Acceleratoe Conference*, Edinburgh, U.K., 26–30 June 2006, pp. 2931–2933.

[46] R. Ryne, *Advanced computing tools and models for accelerator physics*, *Conf. Proc. C* **0806233** (2008) THYM03.

[47] M. Borland, *Simple method for particle tracking with coherent synchrotron radiation*, *Phys. Rev. ST Accel. Beams* **4** (2001) 070701.

[48] D. Sagan, *Bmad: A relativistic charged particle simulation library*, *Nucl. Instrum. Meth. A* **558** (2006) 356.

[49] E.L. Saldin, E.A. Schneidmiller and M.V. Yurkov, *Radiative interaction of electrons in a bunch moving in an undulator*, *Nucl. Instrum. Meth. A* **417** (1998) 158.

[50] D. Sagan and C. Mayes, *Coherent Synchrotron Radiation Simulations for Off-Axis Beams Using the Bmad Toolkit*, in *Proceedings of the 8th International Particle Accelerator Conference*, Copenhagen, Denmark, 14–19 May 2017, pp. 3887–3890.

2021 JINST 16 P10010

[51] *Pulsar website for gpt*, http://www.pulsar.nl/gpt/, 2011.

[52] A.D. Brynes et al., *Beyond the Limits of* 1*D Coherent Synchrotron Radiation*, *New J. Phys.* **20** (2018) 073035 [arXiv:1805.05702].

[53] T. Agoh, *Steady fields of coherent synchrotron radiation in a rectangular pipe*, *Phys. Rev. ST Accel. Beams* **12** (2009) 094402.

[54] A. Novokhatski, *Field dynamics of coherent synchrotron radiation using a direct numerical solution of Maxwell's equations*, *Phys. Rev. ST Accel. Beams* **14** (2011) 060707.

[55] D. Bizzozero, E. Gjonaj and H. De Gersem, *Modeling coherent synchrotron radiation with a discontinuous galerkin time-domain method*, *J. Comp. Phys.* **394** (2019) 745.

[56] M. Dohlus and T. Limberg, *Emittance growth due to wake fields on curved bunch trajectories*, *Nucl. Instrum. Meth. A* **393** (1997) 490.

[57] M. Dohlus and T. Limberg, *CSRtrack: Faster calculations of 3-D CSR effects*, in *Proceedings of the FEL2004 Conference*, Trieste, Italy, 29 August–3 September 2004, pp. 18–21.

[58] M. Dohlus, A. Kabel and T. Limberg, *Efficient field calculation of 3-D bunches on general trajectories*, *Nucl. Instrum. Meth. A* **445** (2000) 338.

[59] M. Dohlus, *Two methods for the calculation of CSR fields*, Tech. Rep., DESY-TESLA-FEL-2003-05 (2003).

[60] G. Bassi, J.A. Ellison, K. Heinemann and R. Warnock, *Microbunching Instability in a Chicane: Two-Dimensional Mean Field Treatment*, *Phys. Rev. ST Accel. Beams* **12** (2009) 080704.

[61] K. Heinemann, D. Bizzozero, J. Ellison, S. Lau and G. Bassi, *Rapid integration over history in self-consistent 2D CSR modeling*, in *Proceedings of the 11th International Computational Accelerator Physics Conference*, Rostock-Warnemuende, Germany, 19–24 August 2012, TUSDC2 [https://accelconf.web.cern.ch/ICAP2012/papers/tusdc2.pdf].

[62] W. Lou and C. Mayes, *WeiyuanLou/PyCSR2D: Second release of PyCSR2D*, https://doi.org/10.5281/zenodo.5496243 (2021).

[63] J. Qiang, S. Lidia, R.D. Ryne and C. Limborg-Deprey, *Three-dimensional quasistatic model for high brightness beam dynamics simulation*, *Phys. Rev. ST Accel. Beams* **9** (2006) 044204 [*Erratum ibid.* **10** (2007) 129901]

[64] C.E. Mitchell, J. Qiang and R.D. Ryne, *A fast method for computing 1-D wakefields due to coherent synchrotron radiation*, *Nucl. Instrum. Meth. A* **715** (2013) 119.

[65] R.D. Ryne, *On FFT-based convolutions and correlations, with application to solving Poisson's equation in an open rectangular pipe*, arXiv:1111.4971.

[66] C.E. Mitchell, J. Qiang, R.D. Ryne, B.E. Carlsten and N.A. Yampolsky, *Large-scale Simulation of Synchrotron Radiation using a Lienard-Wiechert Approach*, *Conf. Proc. C* **1205201** (2012) 1689.

[67] R. Ryne, B. Carlsten, C. Mitchell and J. Qiang, *Self-Consistent Modeling using a Lienard-Wiechert Particle-Mesh Method*, in *Proceedings of the 9th International Particle Accelerator Conference*, Vancouver, BC, Canada, 29 April–4 May 2018, pp. 3313–3315.

[68] J.L. Synge, *On the electromagnetic two-body problem*, *Proc. Roy. Soc. London A* **177** (1940) 118.

[69] C. Mayes, *ChristopherMayes/PyCSR3D: PyCSR3D version 0.2.0*, https://doi.org/10.5281/zenodo.5496096 (2021).

[70] C. Mayes, *ChristopherMayes/OpenCSR: OpenCSR v0.1.1*, https://doi.org/10.5281/zenodo.5165758 (2021).

[71] M. Frigo and S.G. Johnson, *The design and implementation of FFTW3*, *Proc. IEEE* **93** (2005) 216.

[72] D. Sagan et al., *Simulations of Future Particle Accelerators: Issues and Mitigations*, 2021 *JINST* **16** T10002, [arXiv:2108.11027].

[73] D.J. Griffiths, T.C. Proctor and D.F. Schroeter, *Abraham-Lorentz versus Landau-Lifshitz*, *Am. J. Phys.* **78** (2010) 391.